NIH Public Access
Author Manuscript
Adv Biol Regul. Author manuscript; available in PMC 2015 January 01.

Published in final edited form as:
Adv Biol Regul. 2014 January ; 54: 74–91. doi:10.1016/j.jbior.2013.10.002.

Insights into mRNA export-linked molecular mechanisms of human disease through a Gle1 structure-function analysis

Andrew W. Folkmann, **T. Renee Dawson**, and **Susan R. Wente***
Department of Cell and Developmental Biology, Vanderbilt University School of Medicine, U-3207A MRBIII, Nashville, TN 37232—8240 USA

Abstract

A critical step during gene expression is the directional export of nuclear messenger (m)RNA through nuclear pore complexes (NPCs) to the cytoplasm. During export, Gle1 in conjunction with inositol hexakisphosphate (IP_6) spatially regulates the activity of the DEAD-box protein Dbp5 at the NPC cytoplasmic face. *GLE1* mutations are causally linked to the human diseases lethal congenital contracture syndrome 1 (LCCS1) and lethal arthrogryposis with anterior horn cell disease (LAAHD). Here, structure prediction and functional analysis provide strong evidence to suggest that the LCCS1 and LAAHD disease mutations disrupt the function of Gle1 in mRNA export. Strikingly, direct fluorescence microscopy in living cells reveals a dramatic loss of steady-state NPC localization for GFP-gle1 proteins expressed from human *gle1* genes harboring LAAHD and LCCS1 mutations. The potential significance of these residues is further clarified by analyses of sequence and predicted structural conservation. This work offers insights into the perturbed mechanisms underlying human LCCS-1 and LAAHD disease states and emphasizes the potential impact of altered mRNA transport and gene expression in human disease.

Introduction

Proper eukaryotic gene expression requires multiple, highly orchestrated events centering on the fate of the transcribed messenger RNA (mRNA): from transcription to translation to degradation. At the core of this regulation are RNA binding proteins (RBPs) that associate with each mRNA transcript to form a messenger ribonucleoprotein (mRNP) complex. Throughout its lifecycle, each mRNP undergoes a series of dynamic changes to its RBP composition that mediate specific functions such as splicing, nuclear export, translation, and degradation (McKee et al., 2007, Muller-McNicoll et al., 2013). Considering elaborate networks of RNA/protein and protein/protein interactions are coordinated to regulate RNA metabolism, it is expected that perturbing these interactions can have complex, if not pleiotropic, cellular phenotypes. Indeed, alterations in RBPs or factors that influence RBP function have been linked to many human disease states (Cooper et al., 2009, Hurt et al., 2008, Renoux et al., 2012). These pathologies cover a broad spectrum of tissues, organs, age onset, and severity of phenotype. Although causative biochemical and cellular alterations are known for some of these genetic linkages, the molecular mechanisms underlying many such deleterious diseases are poorly understood.

© 2013 Elsevier Ltd. All rights reserved.

*Corresponding author: Tel: +1 615 936 3443: fax: +1 615 936 3439. susan.wente@vanderbilt.edu (S. R. Wente).

Publisher's Disclaimer: This is a PDF file of an unedited manuscript that has been accepted for publication. As a service to our customers we are providing this early version of the manuscript. The manuscript will undergo copyediting, typesetting, and review of the resulting proof before it is published in its final citable form. Please note that during the production process errors may be discovered which could affect the content, and all legal disclaimers that apply to the journal pertain.

NIH-PA Author Manuscript
NIH-PA Author Manuscript
NIH-PA Author Manuscript

NIH-PA Author Manuscript

NIH-PA Author Manuscript

NIH-PA Author Manuscript

During the mRNA life cycle, mRNP compositional changes are dictated by the active binding and release of specific RBPs in a process collectively termed RNP remodeling. In several cases, this process is mediated by members of the RNA-dependent ATPase family termed DEAD-box proteins (DBP). The DBP enzymes drive mRNP remodeling through ATP hydrolysis-induced conformational changes that alter the DBP binding to RNA and coincidently RNA-protein interactions (Folkmann et al., 2011, Jankowsky, 2011, Jankowsky et al., 2006, Jankowsky et al., 2007, Rocak et al., 2004). Interestingly, some DBPs require a protein cofactor to stimulate and regulate their activity (Alcazar-Roman et al., 2006, Ballut et al., 2005, Bolger et al., 2011, Korneeva et al., 2005, Nielsen et al., 2009, Rogers et al., 2001, Weirich et al., 2006, Wolf et al., 2010, Yang et al., 2003). This article focuses on the essential, conserved protein Gle1 that is required for modulating distinct DBPs during mRNA export and translation. A convergence of recent studies has revealed detailed models of Gle1 action at the nuclear pore complex (NPC) during mRNA export (Alcazar-Roman et al., 2006, Folkmann et al., 2013, Folkmann et al., 2011, Hodge et al., 2011, Montpetit et al., 2011, Noble et al., 2011, Tran et al., 2007, Weirich et al., 2006). Moreover, a molecular understanding of how Gle1 function is perturbed in a lethal human disease has been elucidated (Folkmann et al., 2013). This work is summarized and a further analysis of other Gle1 perturbations underlying human disease is presented. Taken together, these data indicate that both LCCS-1 and LAAHD disease pathologies precipitate from defective Gle1 function during the export of mRNA through NPCs.

Structure-function analysis of Gle1, a multifunctional regulator of gene expression

By directly regulating the ATPase activity of distinct DBPs at different stages of RNA metabolism, Gle1 is positioned as a global modulator of gene expression (Alcazar-Roman et al., 2006, Bolger et al., 2011, Weirich et al., 2006). Historically, studies to characterize these regulatory roles have focused on the human (h) Gle1 and *Saccharomyces cerevisiae* (y) Gle1 orthologues (Figure 1) (Murphy et al., 1996, Watkins et al., 1998). Further studies have also identified additional Gle1 orthologues in *S. pombe*, *A. thaliana* and *D. rerio* (Braud et al., 2012, Jao et al., 2012, Moon et al., 1998). Conservation of Gle1 polypeptides was first demonstrated by multiple sequence alignment of orthologues from fungi to mammals (Alcazar-Roman et al., 2010, Watkins et al., 1998). Additionally, analysis of yGle1 and hGle1 chimeras has demonstrated a striking degree of functional complementation, providing further evidence of conservation (Watkins et al., 1998). Overall, a highly complementary approach utilizing the strengths of both human and yeast model systems has built a rich molecular and cellular understanding of Gle1's roles during gene expression (Alcazar-Roman et al., 2010, Bolger et al., 2008, Bolger et al., 2011, Folkmann et al., 2013, Hodge et al., 2011, Kendirgi et al., 2003, Kendirgi et al., 2005, Montpetit et al., 2011, Murphy et al., 1996, Noble et al., 2011, Rayala et al., 2004, Watkins et al., 1998, Weirich et al., 2006). While technical restraints have limited a completely parallel or duplicative analysis in both these model systems, each has provided essential insight into the Gle1 function. Specifically, x-ray crystallographic and biochemical analysis of yGle1 have yielded valuable details of molecular interactions, whereas the use of human cell lines has provided insight into the cellular dynamics of hGle1. Although studies have highlighted potential subtle differences between orthologues, the high degree of sequence and functional conservation infers that Gle1 proteins across different phyla operate via a common molecular paradigm.

Identified in a *S. cerevisiae* synthetic lethal screen with a *nup100Δ* mutant strain, Gle1 (GLFG lethal mutant complementation group 1) was originally documented as an essential mRNA export factor (Murphy et al., 1996). Several studies in human cells have since

NIH-PA Author Manuscript

NIH-PA Author Manuscript

NIH-PA Author Manuscript

demonstrated that the function in mRNA export is fully conserved (Kendirgi et al., 2003, Kendirgi et al., 2005, Watkins et al., 1998). Overall, the domain topology of hGle1B and yGle1 is generally shared (Figure 1), although alternative splicing produces two hGle1 isoforms: hGle1B is larger and spans 1-698 amino acid residues, whereas hGle1A lacks the proximal carboxyl (C)-terminal domain (from 655 to 698 residues) (Kendirgi et al., 2003). Both yeast and human proteins localize at steady state to the nuclear rim and specifically to the NPC; however, diffuse cytoplasmic pools are also observed (Kendirgi et al., 2003, Murphy et al., 1996, Strahm et al., 1999). Nucleocytoplasmic shuttling activity is conferred for hGle1 by a 40 amino acid C-terminal region (Kendirgi et al., 2003). While this primary amino acid motif is not conserved in yGle1, immuno-EM analysis shows yGle1 is localized to both sides of the nuclear envelope, suggesting that it also shuttles between the two cellular compartments (Miller et al., 2004).

Targeting of Gle1 to the nuclear rim for mRNA export is achieved through interactions with specific NPC nucleoporins (Nups) on the cytoplasmic fibrils. At its C-terminus, yGle1 binds to yNup42. Likewise, the Nup42 human homologue hCG1 binds the C-terminal domain specific to hGle1B (Figure 1) (Kendirgi et al., 2005, Murphy et al., 1996, Rayala et al., 2004, Strahm et al., 1999, Stutz et al., 1997). Indeed, the hGle1A isoform that lacks the hCG1 binding region shows minimal steady state nuclear rim localization and is predominantly cytoplasmic (Kendirgi et al., 2005). Via a unique amino (N)-terminal 30 amino acid binding site, hGle1 also interacts with hNup155 (Figure 1) (Rayala et al., 2004). A third domain that plays an essential role in Gle1 function and NPC dynamics is a shared predicted coiled-coil domain located in the N-terminal half (Figure 1). Only recently has the function of the coiled-coil domain been determined through extensive structural and biochemical analyses (Folkmann et al., 2013). In both yeast and human cells, the coiled-coil domain mediates self-association into oligomers that can assemble *in vitro* into ~25nm disk-like structures. Oligomerization at the level of at least Gle1 dimers is required only for its localization at the nuclear rim and function during mRNA export, and not for translation. Furthermore, from live cell imaging of hGle1 cellular localization, disruption of hGle1 oligomerization specifically alters its NPC steady-state localization and slows its nucleocytoplasmic shuttling activity required for mRNA export (Folkmann et al., 2013).

At a molecular level, Gle1 functions in mRNA export by regulating the nucleotide-dependent cycle of Dbp5 mRNP remodeling activity (Folkmann et al., 2011, Hodge et al., 2011, Noble et al., 2011). Acting at the terminal step of export, Dbp5 and Gle1 localize to the NPC cytoplasmic face of the NPC through distinct Nup interactions: hDbp5 with hNup214 (yNup159), and hGle1 with hCG1 (yNup42) and hNup155, respectively (Kendirgi et al., 2005, Murphy et al., 1996, Rayala et al., 2004, Schmitt et al., 1999, Strahm et al., 1999, Stutz et al., 1997, Weirich et al., 2004). While it is not fully known how Gle1 oligomerization functions at the NPC, its role in nucleocytoplasmic shuttling indicates that oligomerization might regulate Gle1 residence time at the NPC and alter Gle1 interactions with Dbp5 (Folkmann et al., 2013). With Gle1 and Dbp5 juxtaposed at the NPC, IP_6 plays the critical role of bridging their interaction and thereby promoting an open Dbp5 conformation to allow for efficient loading of ATP and/or RNA (Alcazar-Roman et al., 2010, Montpetit et al., 2011, Noble et al., 2011). Formation of the ATP- and RNA-bound Dbp5 complex then induces a closed conformation that primes the enzyme for ATPase hydrolysis (Mallam et al., 2012). Conversion to the ADP-bound state returns Dbp5 to its open conformation, releases Dbp5 from the RNA, and coincidentally triggers remodeling of the mRNP (Collins et al., 2009, Folkmann et al., 2011, Montpetit et al., 2011, Noble et al., 2011, Tran et al., 2007, von Moeller et al., 2009). Finally, Dbp5 binding to Nup214 facilitates ADP release (Noble et al., 2011), thereby permitting additional rounds of remodeling. These mRNP remodeling events are thought to specifically release the RBPs

NIH-PA Author Manuscript

NIH-PA Author Manuscript

NIH-PA Author Manuscript

required for transit through the NPC, thus acting as a molecular ratchet to impose directionality on nuclear export (Stewart, 2007).

Previous studies have documented that yGle1 also functions in the cytoplasm to regulate translation (Bolger et al., 2008). Specifically, yGle1 in conjunction with IP_6 activates yDbp5's ATPase activity to remodel the mRNP of the translation termination complex (Alcazar-Roman et al., 2010, Bolger et al., 2008). Additionally, yGle1 has a role in translation initiation, acting in this process independently of IP_6 and Dbp5. Here, yGle1 inhibits the ATPase activity of the DBP Ded1, enabling Ded1 to properly control start site selection (Bolger et al., 2011). While a direct role for hGle1 in translation initiation or translation termination has not been documented to date, it has been shown that hGle1 directly interacts with eIF3f, a subunit of the translation initiation machinery (Bolger et al., 2008, Bolger et al., 2011, Rayala et al., 2004). This suggests that the function of Gle1 in translation is also conserved. Interestingly, genetic and functional studies show that yGle1 oligomerization is not required during translation initiation or translation termination. Further studies will be needed to pinpoint the mechanistic basis for Gle1 targeting to the respective translation machineries, and how the mRNP remodeling events during mRNA export and translation are distinct.

The mechanism of Gle1 dysfunction in LCCS-1^{Fin} pathogenesis

The importance of hGle1 function in physiology is clearly illustrated by the autosomal recessive disease Lethal Congenital Contracture Syndrome-1 (LCCS-1) (Nousiainen et al., 2008). An embryonic lethal form of arthrogryposis multiplex congenita (AMC), LCCS-1 pathology is distinguished by total immobility of the fetus. Underlying this phenotype are a lack of anterior horn motor neurons, atrophy of the ventral spinal cord and nearly absent skeletal muscles (Hall, 1985, Herva et al., 1985). In 2008, Nousiainen and colleagues reported a sequence analysis of genomic DNA from LCCS-1 cases that revealed a causal link between the disease and mutation of the *hGLE1* gene. In 51 of 52 cases, the *h-gle1* alleles were homozygous for a single A>G mutation in the third intron of the gene. This homozygous condition is termed *gle1-Fin*$_{Major}$ for its high incidence in the Finnish population, and the mutation generates an illegitimate splice acceptor site that adds nine additional nucleotides to the coding sequence. As such, the *gle1-Fin*$_{Major}$ allele results in an in-frame insertion of a proline-phenylalanine-glutamine (PFQ) tripeptide in the essential N-terminal coiled-coil domain of hGle1 (Figure 1) (Nousiainen et al., 2008). Studies of the *gle1-Fin*$_{Major}$ developmental phenotype in a zebrafish model of Gle1 depletion point to apoptosis of the neuronal precursors as the origin of LCCS-1 motoneuron defects (Jao et al., 2012). However, these zebrafish studies also reveal both neurogenic and non-neurogenic developmental defects with *GLE1* depletion, for which expression of the wild type *hGLE1* rescues but *gle1-Fin*$_{Major}$ does not. From this work, LCCS-1 is likely not a motor neuron specific disease, but rather all organ precursors are probably impacted (Jao et al., 2012).

To shed light on the molecular defect resulting from the PFQ insertion into the hGle1 coiled-coil domain, a combination of cell-based and biophysical analysis has been employed. First, in a siRNA knockdown and Fin$_{Major}$ add-back system in HeLa cells (effectively a mimic of the homozygous recessive situation of LCCS-1^{Fin}), the Fin$_{Major}$ protein is defective in mRNA export and exhibits dramatically slower nucleocytoplasmic shuttling dynamics (Folkmann et al., 2013). In addition, the Fin$_{Major}$ PFQ insertion is predicted to disrupt the coiled-coil domain structure. Indeed, electron microscopy analysis of Fin$_{Major}$ protein shows disorder in the hGle1 oligomeric state (Folkmann et al., 2013). Thus, as oligomerization and the coiled-coil domain are specifically required for mRNA export, gle1-Fin$_{Major}$ protein is perturbed in a critical aspect of hGle1 self-association at the NPC. In sum, the human

NIH-PA Author Manuscript

NIH-PA Author Manuscript

NIH-PA Author Manuscript

LCCS-1^{Fin} disease represents a new molecular disease mechanism wherein mRNP remodeling is altered during export through NPCs.

Investigating connections between Gle1 alterations in LAAHD and the heterozygous form of LCCS-1

In addition to the LCCS-1 pathogenesis for those with homozygous *Fin*$_{Major}$ alleles (designated here LCCS-1^{Fin}), two other mutations have been identified in *hGLE1* with links to the related disease lethal arthrogryposis with anterior horn cell disease (LAAHD) (Nousiainen et al., 2008). LAAHD exhibits a similar but overall milder pathology compared to LCCS-1^{Fin}, with the fetus typically surviving for a short period after birth (Vuopala et al., 1995). In all known LAAHD cases, patients were compound heterozygous for the *Fin*$_{Major}$ mutation and an additional point mutation in the region encoding the C-terminal domain of hGle1. Fifty percent of LAAHD cases screened contained a G>A substitution at nucleotide 1849 in exon 13, converting the encoded valine to a methionine (V617M). The remainder of cases contained a T>C substitution at nucleotide 2051 of exon 16, resulting in an isoleucine to threonine substitution (I684T). Interestingly, a third case of compound heterozygosity with a C-terminal mutation occurred in a single patient whose symptoms were categorized as LCCS-1 (termed here LCCS-1^{Het}). This mutation was observed at nucleotide 1706 in exon 12, encoding a histidine in place of an arginine at residue 569 (R569H) (Nousiainen et al., 2008). Each of these three amino acid substitutions (V617M, I684T, and R569H) apparently imparts very different features to the altered protein at their respective position. However, no studies have been conducted to investigate their perturbations.

Given the pleotropic effects of the disease pathology, we speculated that hGle1 dysfunction resulting from these mutations could be impacting any one or all of the known Gle1 functions. Having determined the molecular defects caused by Fin$_{Major}$ (Folkmann et al., 2013), we investigated the structural and functional perturbations contributed by the C-terminal domain LAAHD and LCCS-1^{Het} disease mutations. As detailed below, sequence and structural comparisons suggested that these changes alter the stability of the C-terminal HEAT repeat domain, hCG1 binding and mRNA export function. Moreover, analysis of the steady-state localization of these *h-gle1* mutants further revealed a disruption in steady state localization to the nuclear rim. Thus, these mutants are likely defective in mRNA export. This is consistent with our previous finding that the Fin$_{Major}$ PFQ-insertion disrupts the function of Gle1 in mRNA export at the NPC.

Results

Homology model of human Gle1B C-terminal domain allows visualization of potential structural characteristics

Each of the mutations contributing to compound heterozygous LAAHD and LCCS-1^{Het} phenotypes occur in the sequence encoding the C-terminal domain of hGle1 (Nousiainen et al., 2008). Previous studies have documented that this domain is necessary and sufficient both for ATPase stimulation of Dbp5 and for binding IP_6 (Alcazar-Roman et al., 2006, Montpetit et al., 2011, Weirich et al., 2006). To gain insight into the functional perturbations contributed by the V617M and I684T modifications in LAAHD as well as the single R569H compound heterozygous case of LCCS-1^{Het}, we examined the spatial location of the disease variants in the context of the C-terminal HEAT repeat folds. To date, an atomic level structural model for any domain of hGle1 has not been reported. However, the crystal structure of the yGle1 C-terminal domain was recently determined (Montpetit et al., 2011), and the yeast C-terminal domain structure is primarily composed of HEAT repeat motifs. To investigate the conservation between yGle1 and hGle1 C-terminal domains, we conducted a

NIH-PA Author Manuscript

NIH-PA Author Manuscript

NIH-PA Author Manuscript

regional sequence alignment for the core region lying between 480–627 for hGle1 and 331–478 for yGle1. This analysis demonstrated a primary sequence identity of 33% and similarity of 57%, excluding loop regions between helices (data not shown). Based on this sequence conservation, we concluded that the crystal structure of yGle1 is a suitable template structure to produce a basic homology model of the hGle1 C-terminal region for the purpose of hypothesis generation.

To generate the model, the amino acid sequence of hGle1(371-627) was submitted to the Phyre-2 protein fold recognition server (Kelley et al., 2009). The server produced three models of greater than 60% confidence in fold homology. As predicted from the sequence conservation between hGle1 and yGle1, the highest scoring model resulted from the threading of hGle1 sequence through the published structure of y-Δ243gle1^{H337R} [PDB 3PEU]. With a reported confidence of 100% and r.m.s.d of 0.7Å, the model predicts that the amino acid sequence of hGle1(371-627) produces an all alpha-helix HEAT repeat fold comparable to that of y-Δ243gle1^{H337R} (Figure 2A–B). The two additional models were generated based on published structures of eIF4G [PDB 2VSX and PDB 1HU3]. The eIF4G structure is composed in part of several HEAT repeat motifs, further supporting the fold recognition represented in the hGle1 model (Marcotrigiano et al., 2001). Taken together, these data indicated that the C-terminal domain of hGle1 is likely comprised of all alpha-helix HEAT repeats.

The yGle1 protein binds to IP_6 via positively charged residues located on the Dbp5/yGle1 binding interface (Alcazar-Roman et al., 2010, Montpetit et al., 2011). In the yGle1 crystal structure, the polar residues His-337/Arg-374/Lys-377/Lys-378 interact with the phosphate groups of IP_6 (Montpetit et al., 2011). Prior reports have documented that these IP_6 coordinating residues are conserved throughout evolution (Alcazar-Roman et al., 2010, Montpetit et al., 2011). We searched for additional polar contacts within the yGle1 structure by examining residues that were within 6Å of the IP_6 phosphate groups. This analysis identified Lys-401 as an additional IP_6 coordinating residue for yGle1. Importantly, structural superposition of the hGle1 model onto the yGle1-IP_6-yDbp5 co-crystal structure (PDB ID 3PEU) revealed spatial conservation of this polar charge with residue Gln-554 in the hGle1(371-627) model (Figure 2D). By analysis of the multiple sequence alignment, we found that the hGle1 residue Gln-554 is located at position n+1 from yGle1 residue Lys-401 (Figure 3C). We speculate that this residue provides additional contacts for coordinating IP_6 (Figure 2C–D). Interestingly, the multiple sequence alignment also revealed that several insect and plant Gle1 proteins did not show charge conservation for the identified IP_6 coordinating residues (His-337/Arg-374/Lys-377/Lys-378/Lys-401) (Figure 3A–C). These data suggested that some Gle1 proteins might have diverged to have different requirements for IP_6 binding or might coordinate IP_6 via different positively charged residues. Future studies are needed to distinguish between these possibilities.

Structural superposition of the hGle1 model onto the yGle1-IP_6-yDbp5 co-crystal structure (PDB ID 3PEU) further revealed an apparent high degree of structural complementarity for the hGle1 model with the Dbp5 and IP_6 binding interface that was experimentally determined for yGle1 (Figure 2C–D). This molecular visualization supports our working hypothesis that hGle1 might coordinate the negatively charged IP_6 molecule using conserved or highly similar molecular contact points. Biochemical experiments designed to examine the effects of charge substitutions (and other mutational analysis) of the IP_6 binding site are needed to validate the hypothesis that yeast and human proteins recognize IP_6 in a common binding model.

NIH-PA Author Manuscript

NIH-PA Author Manuscript

NIH-PA Author Manuscript

Substitution of histidine at Arg-569 of hGle1 is predicted to disrupt a putative intramolecular salt-bridge

Sequence alignment analysis revealed that the hGle1 Arg-569 residue altered in LCCS-1^{Het} is highly conserved throughout evolution; however, the functional significance of this residue was unclear. The Arg-569 residue is located in the helical core of the C-terminal domain structure near the Dbp5-Gle1 interface (Figure 4B). The homologous residue in yGle1 is Arg-417. To understand the structural and functional significance of this position, we mapped Gle1 evolutionary sequence conservation onto the surface of the Δ243gle1^{H337R} structure using the Consurf server (Ashkenazy et al., 2010, Glaser et al., 2003, Landau et al., 2005). This analysis demonstrated that the residues comprising the contact points for the core of the yGle1 C-terminal domain were also the most highly conserved evolutionarily, with yGle1 Arg-417 positioned centrally in the conserved region (Figure 4B, 4D). While the polar side-chain of this Arg-417 was located near both the Dbp5 and IP_6 binding interfaces, it did not make direct contact with either of these molecules in the crystal structure. Thus, we hypothesized that this conserved residue might be important for folding and/or stability of the heat repeat tertiary motif. Further, the high degree of sequence conservation suggested that the yGle1 Arg-417 polar side-chain might form intramolecular electrostatic interactions with surrounding polar residues. Indeed, a highly conserved negative polar side-chain of Glu-340 was located within 3 Å of the Arg-417 side-chain (Figure 4D). This data indicated that the Arg-417 likely forms a hydrogen bond with the Glu-340 residue. Furthermore, the homologous residues in hGle1 were conserved identically (Arg569/Glu-489). The high degree of sequence conservation at these positions inferred that the intramolecular hydrogen bond might also be conserved in hGle1. Taken together, we speculated that this intramolecular hydrogen bond is a conserved determinant for the proper folding of the C-terminal domain of Gle1. Preliminary support for this model with respect to yGle1 can be found in a previous study, which reported that substitution of Glutamine at Arg-417 in yGle1 resulted in the recombinant protein being insoluble (Alcazar-Roman et al., 2010). If the intramolecular salt-bridge is indeed conserved in hGle1, we further posit that substitution of histidine at Arg-569 would disrupt this interaction and lead to instability or misfolding of the hGle1 C-terminal domain.

eIF4G and Gle1 share critical structural characteristics

Others have shown that the yGle1 C-terminal domain is structurally similar to that of eIF4G (14% identity, 4.1 Å r.m.s.d) (Montpetit et al., 2011). Functionally, Gle1 and eIF4G share homologous roles as co-factors for respective DBPs; Gle1 activates the Dbp5 ATPase for remodeling and eIF4G stimulates eIF4A helicase activity (Korneeva et al., 2005, Noble et al., 2011, Rogers et al., 2001, Tran et al., 2007). We hypothesized that if yGle1-Arg-417/Glu-340 residues did in fact form an intramolecular salt-bridge bridge critical to the structural integrity of Gle1, a similar hydrogen bonding pair might also be found in the eIF4G helical structure. To test this, a pairwise structural alignment of y-Δ243gle1^{H337R} (PDB 3PEU) and eIF4G (PDB 2VSX) was conducted using the DaliLite server (Holm et al., 2000). This structural alignment revealed the presence of a predicted salt-bridge in eIF4G between residues Asp-568, Arg-742 and Arg-741, which are located at a similar position in the HEAT repeat structure to the proposed salt bridge in yGle1 (Figure 4E). We concluded that an intramolecular salt-bridge in the core of the HEAT repeat fold is a shared structural determinant for both Gle1 and eIF4G.

We next examined the sequence conservation of the Dbp5 and eIF4A binding interfaces on the respective Gle1 and eIF4G structures. To accomplish this, eIF4G sequence conservation was mapped onto the eIF4G structure (PDB 2VSX) using the Consurf server (Figure 5A). Three residues make contacts with eIF4A (Glu-659, Lys-655, Asn-615) (Schutz et al., 2008). In our conservation analysis, we found strong conservation of these residues as well

NIH-PA Author Manuscript

NIH-PA Author Manuscript

NIH-PA Author Manuscript

as Lys-611 and Arg-609, forming a cluster of polar contacts at the eIF4A binding interface (Figure 5A). In a similar fashion, examination of the yGle1/yDbp5 interface revealed that the yGle1 structure contained an identical spatial motif of similar polar residues (Gln-295, Lys-287, Glu-342, Gln-338, Asn-290) within its C-terminal domain (Figure 5B). This suggested that the binding interfaces for yGle1/yDbp5 and eIF4G/eIF4A share a specific motif of molecular polar contacts. Together, these data further supported the hypothesis that eIF4G and Gle1 have many similar key structural characteristics and might have evolved from a shared ancestral DBP co-factor.

Structural analysis of hGle1 Val-617 reveals linkage to defective mRNA export

We next examined the spatial location within the hGle1(371-629) model of the Val-617 residue changed to methionine in LAAHD. This residue was located near the Dbp5-Gle1 interface but did not make direct contact with Dbp5 (Figure 4A). Based on the fold homology, the Val-617 residue was predicted to be positioned directly behind the alpha-helix that contains the Arg-569 residue (Figure 4A). One possible explanation for the pathological effects for this mutation could be that substitution of methionine at this position might disrupt the helical packing of the HEAT repeat motifs. Sequence alignment analysis revealed that the hGle1 Val-617 residue was in a similar region to Thr-468 residue in yGle1 (Figure 4C). Further, the Thr-468 residue is located behind the helix that contains the hydrogen bond donor residue Arg-417 (Figure 4B, 4D). Previously, a *y-gle1*^{T468I} mutant was found to be a loss-of-function allele, and this allele was originally identified based on a synthetic lethal genetic interaction in combination with a null mutant for *NUP42* (*nup42Δ*) (Stutz et al., 1997). Importantly, these results suggested that altering the structure of yGle1 at this position disrupts its function in mRNA export. We predict that the substitution of methionine at Val-617 results in a loss-of-function phenotype in mRNA export for the *h-gle1*^{V617M} mutant.

The hGle1 Iso-684 residue altered in LAAHD is located in the conserved hCG1 binding domain

Previous reports documented that hGle1 scaffolds to the NPC by binding to both hCG1/Nup42 and Nup155, and more recent works indicates an additional role for the coiled-coil domain and hGle1 self-association (Kendirgi et al., 2005, Murphy et al., 1996, Rayala et al., 2004). These interactions are thought to position Gle1 at the NPC cytoplasmic face to allow for spatial activation of Dbp5's mRNP remodeling activity (Tran et al., 2007). Specifically, residues 559–698 of hGle1B are both necessary and sufficient for the biochemical interaction with hCG1. Deletion of these residues results in the loss steady-state nuclear rim localization and shifts hGle1 localization to the cytoplasm (Kendirgi et al., 2003, Kendirgi et al., 2005). The Iso-684 residue modified to threonine in LAAHD is located in the middle of this hCG1-binding motif. Further, in our analysis, there is high sequence conservation for a non-polar residue at this position (Figure 5C). We hypothesize that substitution of a polar residue for Iso-684 might electrostatically clash with hCG1 residues at the binding interface. Alternatively, a polar residue at this position might cause the hCG1-binding domain to be unfolded. In either case, we concluded that substitution of threonine for Iso-684 probably perturbs the interaction of hGle1B with hCG1.

LAAHD/LCCS-1^{Het} altered proteins do not localize at steady-state to the nuclear rim

Since our *in silico* analysis suggested that all three mutations observed in compound heterozygous cases potentially disrupt the function of hGle1 in mRNA export, we hypothesized that these disease mutants might influence the steady-state localization of Gle1 at the nuclear rim. We compared the subcellular localization of GFP-tagged hGle1 proteins with the respective changes to that of the NPC-associated integral membrane protein

NIH-PA Author Manuscript

NIH-PA Author Manuscript

NIH-PA Author Manuscript

Pom121 in HeLa cells. HeLa cells were co-transfected with plasmids expressing Pom121-mCherry and either GFP-hGle1B, GFP-h-gle1B^{R569H}, GFP-h-gle1B^{V617M}, or GFP-h-gle1B^{I684T}. Twelve hours post-transfection, the steady state localization of the GFP-tagged proteins was examined by live cell direct fluorescence microscopy. Wild-type GFP-hGle1B localized to the nuclear rim, overlapping completely with the Pom121-mCherry. In contrast, the steady-state nuclear rim signal intensity for GFP-h-gle1B^{R569H}, GFP-h-gle1B^{V617V}, and GFP-h-gle1B^{I684T} was reduced (Figure 6). These data indicated that each of these changes disrupts the function of Gle1 in mRNA export possibly by inhibiting localization to the NPC.

hGle1 is in a stable complex at the nuclear pore complex

Analysis of the steady state localization of the LAAHD and LCCS-1^{Het} mutants suggested that they had altered steady state localization at the NPC. Our prior studies show that hGle1B localizes to the nuclear rim and cytoplasm, and shuttles between the nuclear and cytoplasmic compartments (Kendirgi et al., 2003). Thus, separate pools of Gle1 might exist to function exclusively in either mRNA export or translation. To investigate the dynamics of Gle1 at the NPC, fluorescence loss after photobleaching (FRAP) microscopy was performed. HeLa cells were co-transfected with plasmids expressing GFP-hGle1B. Twelve hours post-transfection, the nuclear rims of cells transiently expressing GFP-hGle1B were photobleached and the GFP fluorescence was monitored over time. Strikingly, we observed that GFP-hGle1B fluorescence recovered very slowly (Figure 7A). This indicated that hGle1 is in a stable complex at the NPC. In a previous FRAP microscopy study of the dynamics for GFP-yDbp5 at the NPC, GFP-yDbp5 was dynamically associated with the nuclear rim ($t_{1/2}$ of recovery ~0.8s) (Hodge et al., 2011). To see if hDbp5 behaved similarly, we directly next examined the dynamics of GFP-hDbp5 at the nuclear rim using FRAP microscopy. HeLa cells were co-transfected with plasmids expressing GFP-hDbp5. Twelve hours post-transfection, the nuclear rim of cell transiently expressing GFP-hDbp5 was photobleached and the GFP fluorescence was monitored over time. In contrast to GFP-hGle1B, hDbp5 recovered very fast. The FRAP data set was fit with a one-phase exponential association model (Figure 7B–C). The relative $t_{1/2}$ for GFP-hDbp5 was ~0.8s which directly correlated with the previous yDbp5 measurement. Overall, Dbp5 more transiently associated with the NPC in comparison to its co-factor Gle1 that was in a more stable complex. The disparity of the dynamics of Dbp5 and Gle1 at the NPC is highly intriguing. One possible explanation is that Gle1 is bound at the NPC in a stable oligomeric complex to ensure a sufficiently high concentration for efficient stimulation of Dbp5's remodeling activity. As such, we predict that Gle1 self-association into oligomeric complexes influences its residence time at the NPC. In addition, given that Gle1 also shuttles between the nucleus and cytoplasm, there is the potential for different subcellular pools of Gle1 being involved in distinct steps of the mRNA life cycle and gene expression.

Discussion

During normal gene expression, mRNP remodeling events function as distinct transition points that specify both the fate and function the mRNA (Muller-McNicoll et al., 2013, Valkov et al., 2012). Here we investigated the potential structural and functional perturbations contributed by the unique changes found in the compound heterozygous LAAHD and LCCS-1^{Het}. Analysis of the steady-state localization in living cells revealed that the GFP-h-gle1B^{R569H}, GFP-h-gle1B^{V617M}, and GFP-h-gle1^{I684T} disease proteins have perturbed nuclear rim localization. Furthermore, specific structural perturbations potentially result. Based on *in silico* analysis, the R569H and V617M alterations might disrupt the overall fold of the Gle1 C-terminal domain; furthermore the I684T is positioned to disrupt Gle1 binding with hCG1. Combined with our recently published biochemical and *in vivo*

NIH-PA Author Manuscript

NIH-PA Author Manuscript

NIH-PA Author Manuscript

analysis of the molecular defects caused by Fin_{Major}, we propose a unified model of the molecular disease pathology whereby defective mRNA export at NPCs contributes to both the LCCS-1 and LAAHD disease states. Importantly, dysfunctional remodeling of the mRNP during export has emerged as a new molecular disease mechanism for RNA metabolism-linked disease states.

In addition to the insights from analyzing disease mutants, important information is also gained from comparing conserved and divergent aspects of Gle1 orthologues. Previous sequence alignment and structural analysis suggested that the IP_6 coordinating residues in Gle1 are highly conserved throughout evolution (Alcazar-Roman et al., 2010, Montpetit et al., 2011). This suggested that the IP_6 molecule was stringently required for Gle1's regulatory activity of Dbp5 in most organisms. Our new sequence alignment data allows for flexibility in this regulatory paradigm. Specifically, we document that that several insect and plant Gle1 proteins do not apparently share the charge conservation for the key IP_6 coordinating residues, suggesting that these proteins could function independent of IP_6. In addition, *S. cerevisiae* yDbp5 utilizes Lys-477 and Lys-481 to coordinate IP_6 binding with yGle1 (Figure 1) (Alcazar-Roman et al., 2010). Prior sequence alignment analysis documented that these IP_6 coordinating residues in Dbp5 show moderate charge conservation (Figure 8) (Montpetit et al., 2011). It is important to note that the insect Dbp5 proteins examined do not show charge conservation at Lys-477 or Lys-481 positions. This supports our hypothesis that Dbp5/Gle1 might function independent of IP_6 in some cases. It is unclear why the Gle1 and Dbp5 in some organisms might not utilize IP_6. Interestingly, in plant tissues, IP_6 is present at high concentration and is the principal storage form of phosphorus (Raboy, 2001). Thus, it is intriguing to speculate that this high concentration of IP_6 may be deleterious for regulation of Dbp5 and may represent the reason for why Gle1 functions independent of IP_6 in plants. Comprehensive analysis of the sequence conservation of these IP_6 coordinating residues and binding activity in Gle1 is needed across different evolutionary organism kingdoms and phyla to further our understanding.

It had been previously reported that eIF4G and Gle1 share a similar structural fold, suggesting that eIF4G and Gle1 share a similar ancestral DBP co-factor (Montpetit et al., 2011). Importantly, our *in silico* analysis supports and expands upon this conclusion. Specifically, our analysis demonstrates that eIF4G and Gle1 both harbor a key intramolecular salt-bridge that has the potential to stabilize the overall HEAT repeat fold. Secondly, despite lack of sequence conservation, eIF4G and Gle1 have maintained similar spatial positioning of conserved polar contacts in the binding interface for their respective DBP interaction partners. This suggests that eIF4G and Gle1 utilize similar molecular contact points to regulate their respective DBP. These are important insights into the structural and functional aspects of DBP co-factors and will aid the identification of other putative co-factors that regulate DBPs and/or additional Gle1/eIF4G-like co-factors.

The pathological phenotypes for LCCS-1 and LAAHD are highly pleotropic, affecting multiple tissues and organs (Herva et al., 1985, Nousiainen et al., 2008, Vuopala et al., 1995). This is not necessarily unexpected for a case of defective mRNA export, as multiple defects in gene expression are likely to arise from altering such an essential molecular process. However, it is also perplexing that both LAAHD and LCCS-1 pathologies are manifested at a relatively late stage *in utero*; for example, the $LCCS\text{-}1^{Fin}$ disease results in fetal lethality at ~32 weeks gestation and not earlier (e.g. early embryonic development) (Herva et al., 1985). Different tissues and cell types might elicit different pathologies depending on specific severity of the perturbation in gene expression. It is intriguing to speculate that less severe changes that perturb Gle1 activity to a lesser extent might have specific phenotypes in adults. Further, given that Gle1 is positioned to influence multiple steps during gene expression, the possibility exists for distinct perturbations of Gle1

NIH-PA Author Manuscript

NIH-PA Author Manuscript

NIH-PA Author Manuscript

functions in mRNA export or translation having different pathological outcomes. It is also possible that only certain subcellular pools of Gle1 are impacted in discrete diseases, be it the more stable NPC-associated Gle1 oligomers, the cytoplasmic Gle1A form, the nuclear pool, or an actively shuttling population.

Based on the evidence so far, we conclude that the reported disease perturbations of hGle1 in LCCS-1 and LAADH are all impacting mRNA export. It is possible that alleles specific for Gle1 translation roles might have other pathologies. Interestingly, mutations in *hGLE1* have also been linked to a hand and foot dorsalization disease, but both the physiological and molecular underpinnings of this phenotype are yet to be resolved (Al-Qattan et al., 2012). Given the large spectrum of proteins and signaling factors that regulate each gene expression transition point, we predict that aberrant mRNP remodeling will play a role in other RNA metabolism-linked disease states.

Acknowledgments

We thank members of the Wente laboratory, and Jonathan Sheehan and Eric Dawson (Vanderbilt Center for Structural Biology) for critical discussions regarding these projects. We wish to thank Watson Folk for technical assistance. This work was supported by in part by the NCI Cancer Center Support Grant #P30CA068485 utilizing the Cell Imaging Shared Resource and grants from the NIH to S.R.W. (R37 GM51219) and A.W.F. (F31NS070431), and support from T32CA119925 (to A.W.F.).

References

Al-Qattan MM, Shamseldin HE, Alkuraya FS. Familial dorsalization of the skin of the proximal palm and the instep of the sole of the foot. Gene. 2012; 500:216–9. [PubMed: 22484600]

Alcazar-Roman AR, Bolger TA, Wente SR. Control of mRNA export and translation termination by inositol hexakisphosphate requires specific interaction with Gle1. J Biol Chem. 2010; 285:16683–92. [PubMed: 20371601]

Alcazar-Roman AR, Tran EJ, Guo S, Wente SR. Inositol hexakisphosphate and Gle1 activate the DEAD-box protein Dbp5 for nuclear mRNA export. Nature Cell Biology. 2006; 8:711–6.

Ashkenazy H, Erez E, Martz E, Pupko T, Ben-Tal N. ConSurf 2010: calculating evolutionary conservation in sequence and structure of proteins and nucleic acids. Nucleic Acids Res. 2010; 38:W529–33. [PubMed: 20478830]

Ballut L, Marchadier B, Baguet A, Tomasetto C, Seraphin B, Le Hir H. The exon junction core complex is locked onto RNA by inhibition of eIF4AIII ATPase activity. Nat Struct Mol Biol. 2005; 12:861–9. [PubMed: 16170325]

Bolger TA, Folkmann AW, Tran EJ, Wente SR. The mRNA export factor Gle1 and inositol hexakisphosphate regulate distinct stages of translation. Cell. 2008; 134:624–33. [PubMed: 18724935]

Bolger TA, Wente SR. Gle1 is a multifunctional DEAD-box protein regulator that modulates Ded1 in translation initiation. J Biol Chem. 2011; 286:39750–9. [PubMed: 21949122]

Braud C, Zheng W, Xiao W. LONO1 encoding a nucleoporin is required for embryogenesis and seed viability in Arabidopsis. Plant Physiol. 2012; 160:823–36. [PubMed: 22898497]

Collins R, Karlberg T, Lehtio L, Schutz P, van den Berg S, Dahlgren LG, et al. The DEXD/H-box RNA helicase DDX19 is regulated by an {alpha}-helical switch. J Biol Chem. 2009; 284:10296–300. [PubMed: 19244245]

Cooper TA, Wan L, Dreyfuss G. RNA and disease. Cell. 2009; 136:777–93. [PubMed: 19239895]

Folkmann AW, Collier SA, Zhan X, Aditi, Ohi MD, Wente SR. Gle1 functions during mRNA export in an oligomeric complex that is altered in human disease. Cell. 2013 in press.

Folkmann AW, Noble KN, Cole CN, Wente SR. Dbp5, Gle1-IP_6 and Nup159: a working model for mRNP export. Nucleus. 2011; 2:540–8. [PubMed: 22064466]

NIH-PA Author Manuscript NIH-PA Author Manuscript NIH-PA Author Manuscript

Glaser F, Pupko T, Paz I, Bell RE, Bechor-Shental D, Martz E, et al. ConSurf: identification of functional regions in proteins by surface-mapping of phylogenetic information. Bioinformatics. 2003; 19:163–4. [PubMed: 12499312]

Hall JG. Genetic aspects of arthrogryposis. Clin Orthop Relat Res. 1985:44–53. [PubMed: 3978933]

Herva R, Leisti J, Kirkinen P, Seppanen U. A lethal autosomal recessive syndrome of multiple congenital contractures. Am J Med Genet. 1985; 20:431–9. [PubMed: 3993672]

Hodge CA, Tran EJ, Noble KN, Alcazar-Roman AR, Ben-Yishay R, Scarcelli JJ, et al. The Dbp5 cycle at the nuclear pore complex during mRNA export I: *dbp5* mutants with defects in RNA binding and ATP hydrolysis define key steps for Nup159 and Gle1. Genes Dev. 2011; 25:1052–64. [PubMed: 21576265]

Holm L, Park J. DaliLite workbench for protein structure comparison. Bioinformatics. 2000; 16:566–7. [PubMed: 10980157]

Hurt JA, Silver PA. mRNA nuclear export and human disease. Dis Model Mech. 2008; 1:103–8. [PubMed: 19048072]

Jankowsky E. RNA helicases at work: binding and rearranging. Trends Biochem Sci. 2011; 36:19–29. [PubMed: 20813532]

Jankowsky E, Bowers H. Remodeling of ribonucleoprotein complexes with DExH/D RNA helicases. Nucleic Acids Res. 2006; 34:4181–8. [PubMed: 16935886]

Jankowsky E, Fairman ME. RNA helicases--one fold for many functions. Curr Opin Struct Biol. 2007; 17:316–24. [PubMed: 17574830]

Jao LE, Appel B, Wente SR. A zebrafish model of lethal congenital contracture syndrome 1 reveals Gle1 function in spinal neural precursor survival and motor axon arborization. Development. 2012; 139:1316–26. [PubMed: 22357925]

Kelley LA, Sternberg MJ. Protein structure prediction on the Web: a case study using the Phyre server. Nature protocols. 2009; 4:363–71.

Kendirgi F, Barry DM, Griffis ER, Powers MA, Wente SR. An essential role for hGle1 nucleocytoplasmic shuttling in mRNA export. J Cell Biol. 2003; 160:1029–40. [PubMed: 12668658]

Kendirgi F, Rexer DJ, Alcazar-Roman AR, Onishko HM, Wente SR. Interaction between the shuttling mRNA export factor Gle1 and the nucleoporin hCG1: a conserved mechanism in the export of Hsp70 mRNA. Mol Biol Cell. 2005; 16:4304–15. [PubMed: 16000379]

Korneeva NL, First EA, Benoit CA, Rhoads RE. Interaction between the NH2-terminal domain of eIF4A and the central domain of eIF4G modulates RNA-stimulated ATPase activity. J Biol Chem. 2005; 280:1872–81. [PubMed: 15528191]

Landau M, Mayrose I, Rosenberg Y, Glaser F, Martz E, Pupko T, et al. ConSurf 2005: the projection of evolutionary conservation scores of residues on protein structures. Nucleic Acids Res. 2005; 33:W299–302. [PubMed: 15980475]

Mallam AL, Del Campo M, Gilman B, Sidote DJ, Lambowitz AM. Structural basis for RNA-duplex recognition and unwinding by the DEAD-box helicase Mss116p. Nature. 2012; 490:121–5. [PubMed: 22940866]

Marcotrigiano J, Lomakin IB, Sonenberg N, Pestova TV, Hellen CU, Burley SK. A conserved HEAT domain within eIF4G directs assembly of the translation initiation machinery. Mol Cell. 2001; 7:193–203. [PubMed: 11172724]

McKee AE, Silver PA. Systems perspectives on mRNA processing. Cell Res. 2007; 17:581–90. [PubMed: 17621309]

Miller AL, Suntharalingam M, Johnson SL, Audhya A, Emr SD, Wente SR. Cytoplasmic inositol hexakisphosphate production is sufficient for mediating the Gle1-mRNA export pathway. J Biol Chem. 2004; 279:51022–32. [PubMed: 15459192]

Montpetit B, Thomsen ND, Helmke KJ, Seeliger MA, Berger JM, Weis K. A conserved mechanism of DEAD-box ATPase activation by nucleoporins and InsP6 in mRNA export. Nature. 2011; 472:238–42. [PubMed: 21441902]

Moon D, Bae J, Cho H, Yoon J. The fission yeast homologue of Glel is essential for growth and involved in mRNA expor. J Microbiol. 1998; 46:422–8. [PubMed: 18758733]

NIH-PA Author Manuscript NIH-PA Author Manuscript NIH-PA Author Manuscript

Muller-McNicoll M, Neugebauer KM. How cells get the message: dynamic assembly and function of mRNA-protein complexes. Nat Rev Genet. 2013; 14:275–87. [PubMed: 23478349]

Murphy R, Wente SR. An RNA-export mediator with an essential nuclear export signal. Nature. 1996; 383:357–60. [PubMed: 8848052]

Nielsen KH, Chamieh H, Andersen CB, Fredslund F, Hamborg K, Le Hir H, et al. Mechanism of ATP turnover inhibition in the EJC. RNA. 2009; 15:67–75. [PubMed: 19033377]

Noble KN, Tran EJ, Alcazar-Roman AR, Hodge CA, Cole CN, Wente SR. The Dbp5 cycle at the nuclear pore complex during mRNA export II: nucleotide cycling and mRNP remodeling by Dbp5 are controlled by Nup159 and Gle1. Genes Dev. 2011; 25:1065–77. [PubMed: 21576266]

Nousiainen HO, Kestila M, Pakkasjarvi N, Honkala H, Kuure S, Tallila J, et al. Mutations in mRNA export mediator GLE1 result in a fetal motoneuron disease. Nat Genet. 2008; 40:155–7. [PubMed: 18204449]

Raboy V. Seeds for a better future: 'low phytate' grains help to overcome malnutrition and reduce pollution. Trends Plant Sci. 2001; 6:458–62. [PubMed: 11590064]

Rayala HJ, Kendirgi F, Barry DM, Majerus PW, Wente SR. The mRNA export factor human Gle1 interacts with the nuclear pore complex protein Nup155. Mol Cell Proteomics. 2004; 3:145–55. [PubMed: 14645504]

Renoux AJ, Todd PK. Neurodegeneration the RNA way. Prog Neurobiol. 2012; 97:173–89. [PubMed: 22079416]

Rocak S, Linder P. DEAD-box proteins: the driving forces behind RNA metabolism. Nat Rev Mol Cell Biol. 2004; 5:232–41. [PubMed: 14991003]

Rogers GW Jr, Richter NJ, Lima WF, Merrick WC. Modulation of the helicase activity of eIF4A by eIF4B, eIF4H, and eIF4F. J Biol Chem. 2001; 276:30914–22. [PubMed: 11418588]

Schmitt C, von Kobbe C, Bachi A, Pante N, Rodrigues JP, Boscheron C, et al. Dbp5, a DEAD-box protein required for mRNA export, is recruited to the cytoplasmic fibrils of nuclear pore complex via a conserved interaction with CAN/Nup159p. EMBO J. 1999; 18:4332–47. [PubMed: 10428971]

Schutz P, Bumann M, Oberholzer AE, Bieniossek C, Trachsel H, Altmann M, et al. Crystal structure of the yeast eIF4A-eIF4G complex: an RNA-helicase controlled by protein-protein interactions. Proc Natl Acad Sci U S A. 2008; 105:9564–9. [PubMed: 18606994]

Stewart M. Ratcheting mRNA out of the nucleus. Mol Cell. 2007; 25:327–30. [PubMed: 17289581]

Strahm Y, Fahrenkrog B, Zenklusen D, Rychner E, Kantor J, Rosbach M, et al. The RNA export factor Gle1p is located on the cytoplasmic fibrils of the NPC and physically interacts with the FG-nucleoporin Rip1p, the DEAD-box protein Rat8p/Dbp5p and a new protein Ymr 255p. EMBO J. 1999; 18:5761–77. [PubMed: 10610322]

Stutz F, Kantor J, Zhang D, McCarthy T, Neville M, Rosbash M. The yeast nucleoporin rip1p contributes to multiple export pathways with no essential role for its FG-repeat region. Genes Dev. 1997; 11:2857–68. [PubMed: 9353255]

Tran EJ, Zhou Y, Corbett AH, Wente SR. The DEAD-box protein Dbp5 controls mRNA export by triggering specific RNA:protein remodeling events. Mol Cell. 2007; 28:850–9. [PubMed: 18082609]

Valkov E, Dean JC, Jani D, Kuhlmann SI, Stewart M. Structural basis for the assembly and disassembly of mRNA nuclear export complexes. Biochim Biophys Acta. 2012; 1819:578–92. [PubMed: 22406340]

von Moeller H, Basquin C, Conti E. The mRNA export protein DBP5 binds RNA and the cytoplasmic nucleoporin NUP214 in a mutually exclusive manner. Nature structural & molecular biology. 2009; 16:247–54.

Vuopala K, Ignatius J, Herva R. Lethal arthrogryposis with anterior horn cell disease. Hum Pathol. 1995; 26:12–9. [PubMed: 7821908]

Watkins JL, Murphy R, Emtage JL, Wente SR. The human homologue of *Saccharomyces cerevisiae* Gle1p is required for poly(A)+ RNA export. Proc Natl Acad Sci U S A. 1998; 95:6779–84. [PubMed: 9618489]

NIH-PA Author Manuscript

NIH-PA Author Manuscript

NIH-PA Author Manuscript

Weirich CS, Erzberger JP, Berger JM, Weis K. The N-terminal domain of Nup159 forms a beta-propeller that functions in mRNA export by tethering the helicase Dbp5 to the nuclear pore. Mol Cell. 2004; 16:749–60. [PubMed: 15574330]

Weirich CS, Erzberger JP, Flick JS, Berger JM, Thorner J, Weis K. Activation of the DExD/H-box protein Dbp5 by the nuclear-pore protein Gle1 and its coactivator InsP6 is required for mRNA export. Nat Cell Biol. 2006; 8:668–76. [PubMed: 16783364]

Wolf A, Krause-Gruszczynska M, Birkenmeier O, Ostareck-Lederer A, Huttelmaier S, Hatzfeld M. Plakophilin 1 stimulates translation by promoting eIF4A1 activity. J Cell Biol. 2010; 188:463–71. [PubMed: 20156963]

Yang HS, Jansen AP, Komar AA, Zheng X, Merrick WC, Costes S, et al. The transformation suppressor Pdcd4 is a novel eukaryotic translation initiation factor 4A binding protein that inhibits translation. Mol Cell Biol. 2003; 23:26–37. [PubMed: 12482958]

NIH-PA Author Manuscript

NIH-PA Author Manuscript

NIH-PA Author Manuscript

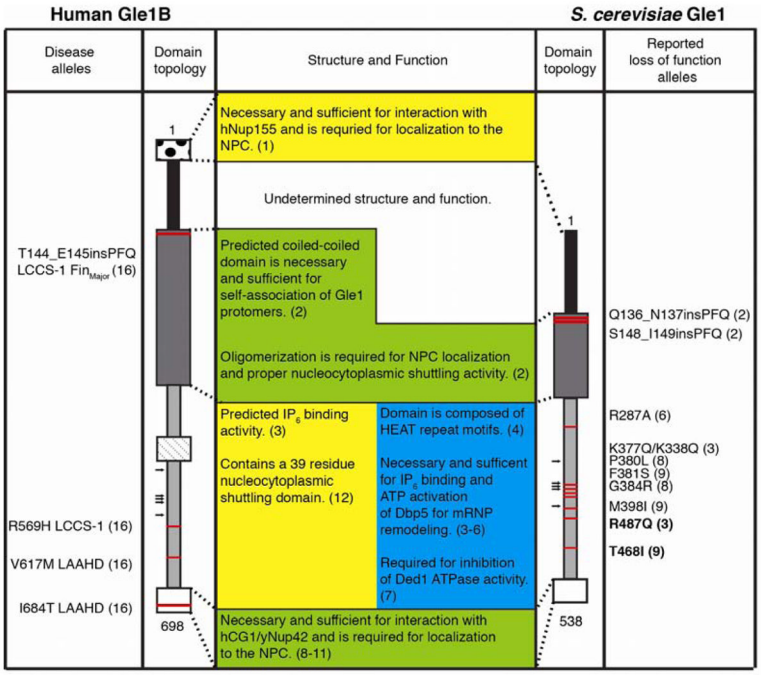

Fig. 1.

Schematic depicting functional and structural domains of Human (Left) and *S. Cerevisiae* (Right) Gle1 proteins is shown. Red dashes indicate the relative position of indicated *gle1* alleles. Black arrows mark the location of the conserved IP_6-coordinating residues. References cited: (1) Rayala et al., 2004 (2) Folkmann et al., 2013 (3) Alcazar-Roman et al., 2010 (4) Montpetit et al., 2011 (5) Tran et al., 2007 (6) Weirich et al., 2006, Alcazar-Roma et al., 2010 (7) Bolger and Wente, 2011 (8) Murphy and Wente, 1996 (9) Stutz et al., 1997 (10) Strahm et al., 1999 (11) Kendirgi et al., 2005 (12) Kendirgi et al., 2003 (13) Nousianinen et al., 2008.

NIH-PA Author Manuscript

NIH-PA Author Manuscript

NIH-PA Author Manuscript

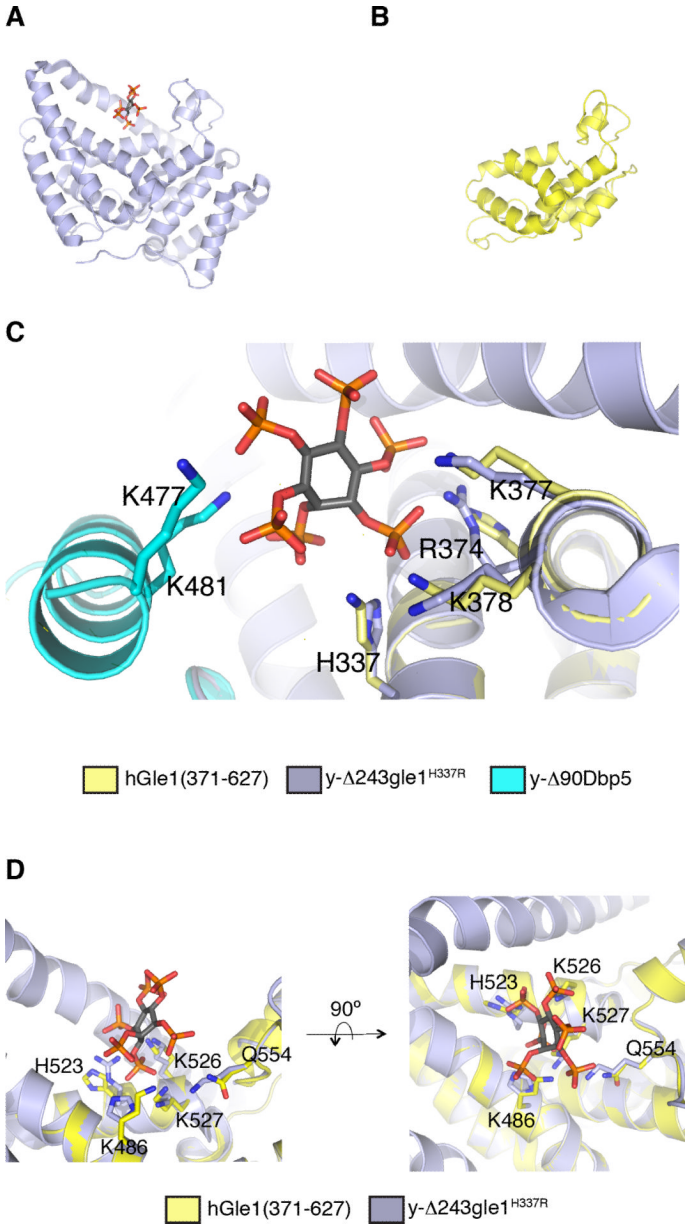

Fig. 2.

Identification of putative IP_6 coordinating residues in hGle1. (A) Structure of y-Δ243gle1^{H337R} (GRAY) [PDB 3PEU] is shown. (B) A homology model for hGle1(371-627) (YELLOW) was generated based on the crystal structure of y-Δ243gle1^{H337R} [PDB 3PEU] using the structure prediction server Phyre-2 (Keley and Sternberg, 2009). (C–D) This model was constructed by superposing the hGle1(371-627) model onto the y-Δ243gle1^{H337R} molecule within the y-Δ90dbp5/y-Δ243gle1^{H337R} complex (PDB 3PEU). IP_6 is rendered as a gray stick molecule with orange phosphate and red oxygen atoms. Nitrogen atoms in Gle1 structures are in blue. (C) Conserved IP_6-coordinating polar residues in yGle1 and yDbp5 are labeled. (D) Conserved polar residues in hGle1 are labeled. Methods: Structural analysis and generation of the figure images was done using the program PyMOL (Schrödinger, Inc).

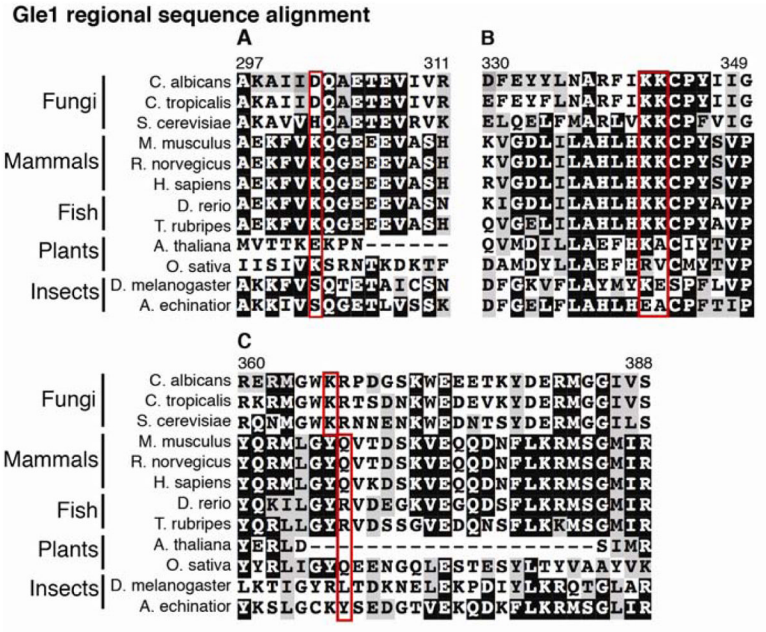

Fig. 3.

Charge conservation of the IP_6 coordinating residues in Gle1 is observed in some organisms (A–C) Sequence alignment of conserved region of the C-terminal domain of Gle1 from selected fungal and metazoan species. (A) Red box indicates position of yGle1-H337 and hGle1-K486 residues. (B) Red box indicates position of yGle1-R374/K377/K378 and hGle1-H523/K526/K527 residues. (C) Red box indicates position of yGle1-K401 and hGle1-Q554 residues.

NIH-PA Author Manuscript NIH-PA Author Manuscript NIH-PA Author Manuscript

NIH-PA Author Manuscript

NIH-PA Author Manuscript

NIH-PA Author Manuscript

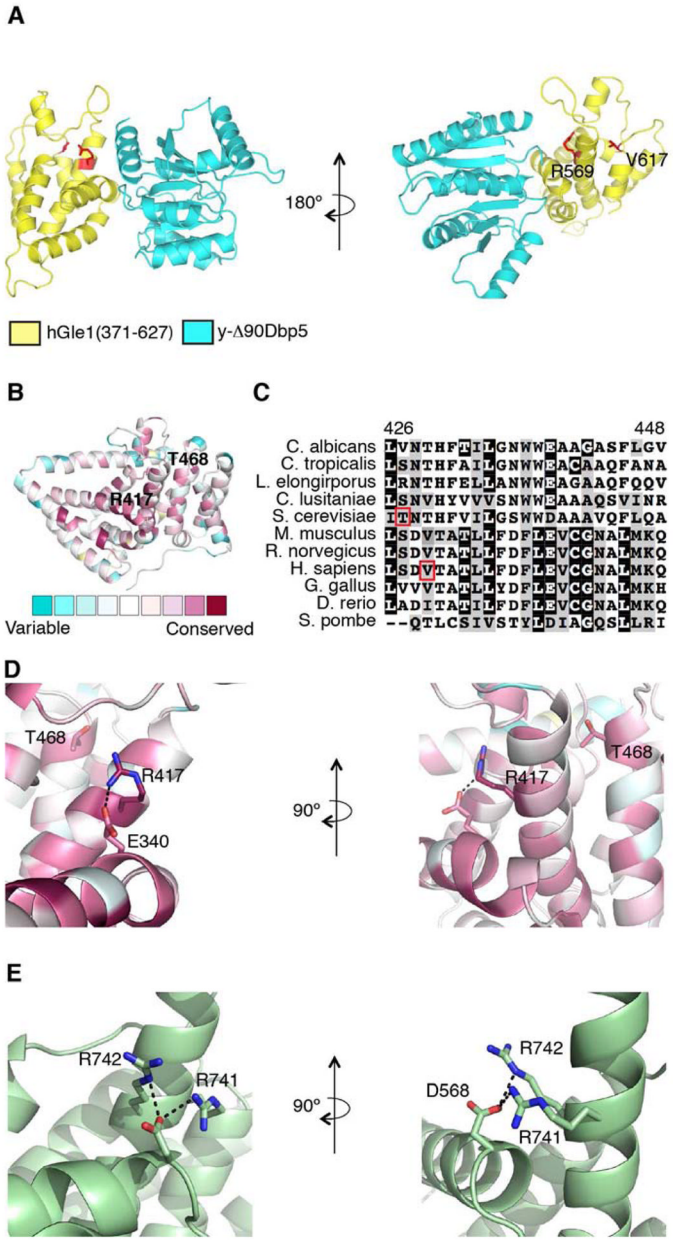

Fig. 4.

Conservation of intramolecular salt-bridge in yGle1 and eIF4G. (A) This model was constructed by replacing the y-Δ243gle1^{H337R} molecule within the y-Δ90dbp5/y-Δ243 gle1^{H337R} complex (PDB 3PEU) with the homology model of hGle1(371-627). (B) The results of the analysis of the y-Δ241gle1^{H337R} by the ConSurf server are shown. The Gle1 structure is represented by a ribbon model, colored by the following conservation scale: dark purple residues are the most conserved; white residues are the average on the conservation scale; cyan residues are variable. (C) Sequence alignment of conserved region of the C-terminal domain of Gle1 from selected fungal and metazoan species. Sequences were aligned with ClustalX, shaded with Boxshade 2.1. Red boxes denote the positions of Thr-468 and Val-617 residues in yeast and human Gle1 respectively. (D) Conserved residues in y-Δ243gle1^{H337R} structure are depicted. Dashed line indicated potential

NIH-PA Author Manuscript

NIH-PA Author Manuscript

NIH-PA Author Manuscript

hydrogen bond (distance <3Å). (E) Hydrogen bond acceptor and donor residues are indicated in eIF4G structure (PDB 2VSX). Dashed line indicates potential hydrogen bond (distance <3Å). Methods: Structural analysis and generation of the figure images was done using the program PyMOL (Schrödinger, Inc). Multiple sequence alignment analysis was done using the ClustalX, and shaded with Boxshade 3.21

NIH-PA Author Manuscript

NIH-PA Author Manuscript

NIH-PA Author Manuscript

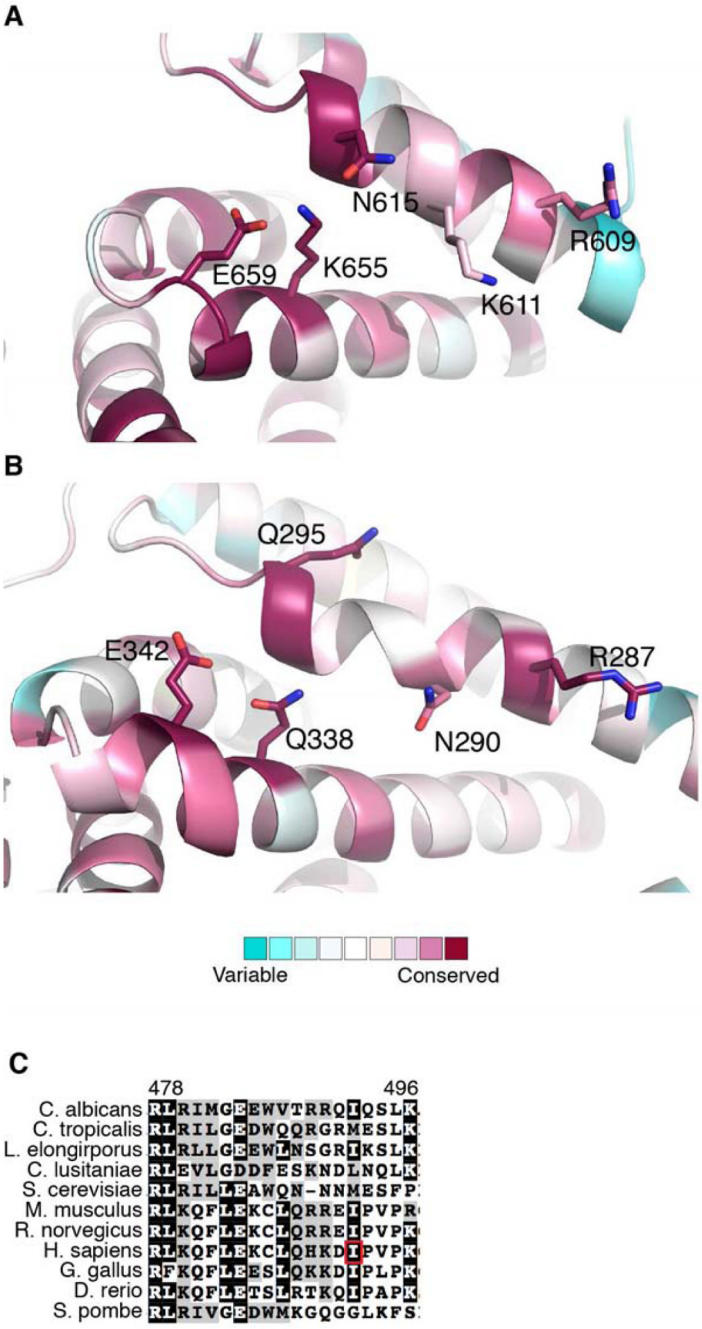

Fig. 5.

Conservation of molecular polar contact points in Gle1 and eIF4G. (A–B) The results of the analysis of the (B) y-Δ243gle1^{H337R} [PDB 3PEU] and (C) eIF4G [PDB 2VSX] structures by the ConSurf server are shown. A ribbon model is depicted, colored by the following conservation scale, represents the structures: dark purple residues are the most conserved; white residues are the average on the conservation scale; cyan residues are variable. Conserved polar residues for yGle1 and eIF4G are labeled. (C) Sequence alignment of conserved region of the C-terminal domain of Gle1 from selected fungal and metazoan species. Sequences were aligned with ClustalX, shaded with Boxshade 2.1. Red box denotes the position of the Iso-684 hGle1B residue. Methods: Structural analysis and generation of

NIH-PA Author Manuscript

NIH-PA Author Manuscript

NIH-PA Author Manuscript

the figure images was done using the program PyMOL (Schrödinger, Inc). Multiple sequence alignment analysis was done using the ClustalX, and shaded with Boxshade 3.21

NIH-PA Author Manuscript

NIH-PA Author Manuscript

NIH-PA Author Manuscript

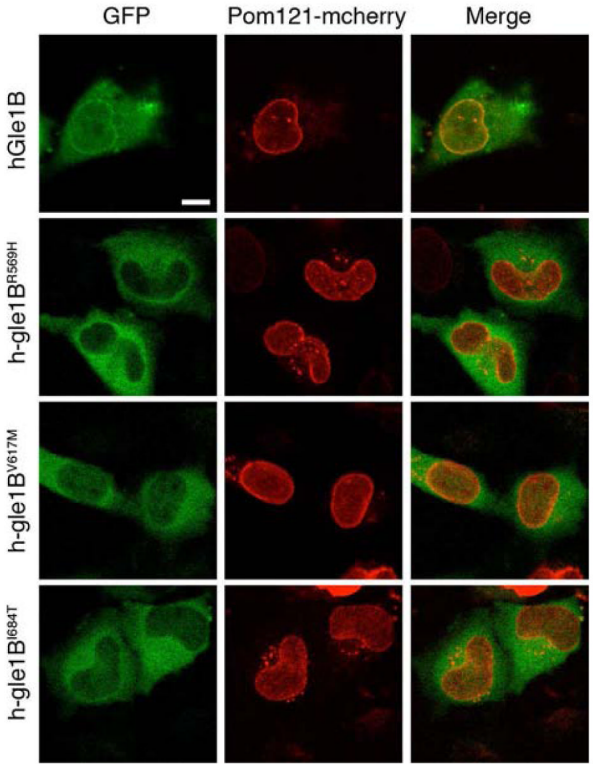

Fig. 6.

LAAHD and LCCS-1^{Het} Gle1 proteins have altered steady-state NPC localization. HeLa cells expressing *POM121-mCherry* and either *GFP-hGLE1B*, *GFP-h-gle1B*^{R569H}, *GFP-h-gle1B*^{V617M}, and *GFP-h-gle1B*^{I684T} were visualized by direct fluorescent live cell microscopy. Bar, 10 μm. Methods: Hela cells were cultured in complete medium (DMEM, Gibco) supplemented with 10% FBS (Alanta Biologicals) at 37 °C in 5% CO_2. Cells were plated in 35mm No. 1.5 glass bottom dishes (Mattek). Transient transfection with indicated plasmids was performed using Fugene6 (Promega) following manufacturer recommendations: *POM121-mCherry* and pSW1831 (*GFP-hGle1B*), pSW3971 (*GFP-h-gle1B*^{R569H}), pSW3972 (*GFP-h-gle1B*^{V617M}), or pSW3973 (*GFP-h-gle1B*^{I684T}). All live-cell direct fluorescence microscopy experiments were performed on a confocal microscope (LSM710, Zeiss, 40X/1.1 C-Apochromat water objective).

NIH-PA Author Manuscript

NIH-PA Author Manuscript

NIH-PA Author Manuscript

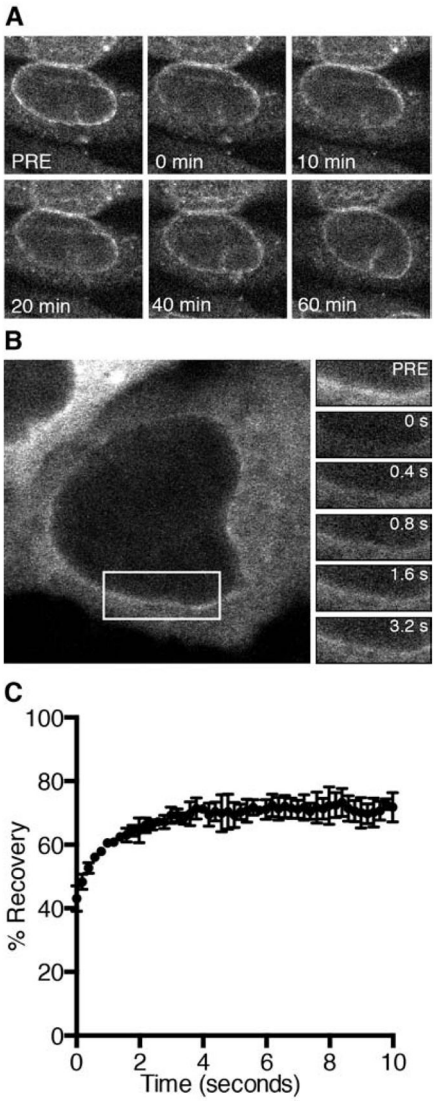

Fig. 7.

Gle1 is a stable component of the NPC. (A) HeLa cells expressing *GFP-hGLE1B* were analyzed by FRAP microscopy. Representative nuclear rim FRAP time series images are shown. Bar, 10 μm. (B) HeLa cells expressing *GFP-hDBP5* were analyzed by FRAP microscopy. Representative nuclear rim FRAP time series images are shown. Bar, 10 μm. White box indicates imaging region of interest for FRAP acquisition (C) FRAP recovery curve experimental determined bleached region, fit with a one-phase association model. Error bars represent mean ± standard deviation with n=5 cells. Methods: HeLa cells were cultured and transfected as in Figure 4. FRAP microscopy experiments were performed on HeLa cells co-transfected with *POM121-mCherry* and either pSW1832, or pSW3253 (*GFP-hDBP5*). The bleaching region of interest (B-ROI) was set to encompass the nuclear rim. Bleaching was achieved by exciting at 488 nM throughout the entire B-ROI (with a LSM710, Zeiss, 40X/1.1 C-Apochromat water objective). Post-bleaching images were acquired every 10 minutes (GFP-hGle1) or 200ms (GFP-hDbp5).

NIH-PA Author Manuscript

NIH-PA Author Manuscript

NIH-PA Author Manuscript

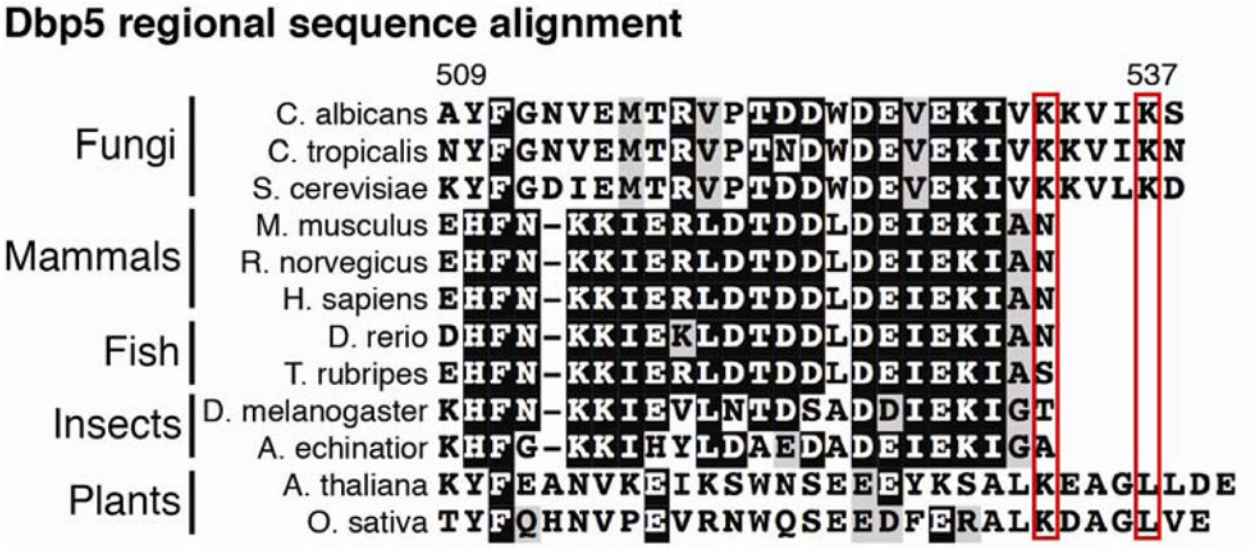

Fig. 8.

Charge conservation of the IP_6 coordinating residues in Dbp5 is observed in some organisms. (A) Sequence alignment of the far C-terminal region in Dbp5 from selected fungal and metazoan species. Red box indicates position of yDbp5-K477/K481 residues.